ICARUS 105, 363–369 (1993)

Size Distributions of Satellite Dust Ejecta: Effects of Radiation Pressure and Planetary Oblateness

ROBIN M. CANUP, JOSHUA E. COLWELL, AND MIHALY HORANYI

Laboratory for Atmospheric and Space Physics, University of Colorado, Box 392, Boulder, Colorado 80309-0392
E-mail: canup@sargon.colorado.edu

Received May 10, 1993; revised August 4, 1993

We examine the steady-state size distribution of dust ejecta in the vicinity of a satellite which acts as both a source and a sink for dust particles. The orbital motion of the dust particles is modified by radiation pressure and planetary oblateness which together produce periodic eccentricity perturbations. Our numerical simulations show that these perturbations can lead to a steepening of the steady-state power-law size distribution such that the index increases by 1 from the index of the source distribution in a specific size regime. This regime is determined by the perturbation strength, and the size and orbital radius of the satellite. The steady-state size distribution is reached in 10–20 years for the conditions considered here. In general, the perturbations discussed here affect dust particle orbits on shorter time scales than Poynting–Robertson, exospheric, or plasma drag forces. © 1993 Academic Press, Inc.

I. INTRODUCTION

Dust particles ejected from satellites near ring systems are believed to be a source of material for ethereal rings and dust bands (e.g., Soter 1971, Burns *et al.* 1980, Colwell and Esposito 1990a,b, Banaszkiewicz and Ip 1991, Juhász *et al.* 1993). Such a source is necessary to sustain the existence of these structures against various destructive forces (e.g., Burns *et al.* 1980). The study of the orbital evolution and the eventual fate of these particles represents a crucial link in the understanding of the origin and evolution of dusty planetary rings. In this paper, we examine the effect of two perturbations, radiation pressure and planetary oblateness, on the orbits of particles ejected from small satellites and the steady-state distribution of dust in the region of the satellite. Other perturbations modify the orbits of particles considered here on much longer time scales than those relevant to this work, and are ignored.

We calculate the steady-state size distribution of orbiting dust which results from the balance of a continuous ejecta supply and loss by reimpact with the parent body or bodies. The sweep up of dust grains through reimpact is a function of the evolving eccentricity of the dust particles. Specifically, we study the steady-state dust distributions that coexist with small satellites in orbit near the ring of Jupiter. While Jupiter's obliquity is very small (about 3°), the more significant obliquities of the other giant planets (ranging from 26° to 97°) will produce a periodic forcing of dust particle inclinations that is not included in this initial study. We therefore consider the orbital evolution of ejected dust particles only for satellites in the jovian system. We ignore loss of dust particles due to drag processes or catastrophic fragmentation, since for 1- to 1000-μm radius grains these processes operate on much longer time scales that those examined here. We also neglect charge effects (relatively unimportant for particles greater than 10 μm in radius) and perturbations due to passage through the planet's shadow.

We show that the orbital modifications resulting from the effects of radiation pressure and planet oblateness lead to distinct modifications of the steady-state size distribution from that in the nonperturbed case for dust grains on low-eccentricity orbits. These perturbations affect the eccentricities of small grains as a function of grain size. Collision frequencies vary with eccentricity in such a way that the resulting size distribution is steeper than the source distribution. This is the only mechanism we are aware of that could lead to a steepening, rather than a flattening, of planetary ring size distributions. This mechanism may contribute to the observed steep size distribution of dust in Saturn's G ring (Showalter and Cuzzi 1993), although more detailed modeling is necessary.

II. NUMERICAL MODEL

II.1. Source of Ejecta

We parameterize the production of dust from micrometeoroid impacts by an impact flux, F_μ, that is assumed constant in time, and a characteristic yield, Y, that is a function of target surface properties. The yield is defined by $Y = M_{ej}/M_\mu$ where M_{ej} is the total mass of the ejecta

0019-1035/93 $5.00

produced by an impactor of mass M_μ. Since we are considering the steady-state size distribution of dust on short time scales, we ignore the less frequent impacts of large meteoroids. The number of mass m particles produced in time Δt is then

$$\Delta n_m = \frac{F_\mu f_g \pi R^2 Y n(m)}{M_{ej}} \Delta t. \quad (1)$$

The flux is enhanced by the gravitational focusing term, $f_g = 1 + (GM_{plan}/(v_\infty^2\, a))$ (Morfill *et al.* 1983), R is the radius of the satellite, and $n(m)$ is the number of mass m ejecta particles produced in a single impact. Because we use a discrete logarithmic mass vector binned by factors of two in mass (below), the quantity $n(m)/M_{ej}$ in Eq. (1) can be expressed as

$$n(m)/M_{ej} = \frac{m^{1-q_m}(2^{1-q_m} - 1)(2 - q_m)}{(1 - q_m)(m_{max}^{2-q_m} - m_{min}^{2-q_m})}, \quad (2)$$

where m_{min}, m_{max}, and q_m are, respectively, the lower and upper mass cutoffs and the differential mass power-law index of the ejecta mass distribution. We use a value of 10^{-16} gm cm^{-2} sec^{-1} for F_μ (Cuzzi and Durisen 1990), and for Y we use 10^4, appropriate for impacts onto hard (basalt) target materials (Burns *et al.* 1984). These values are reasonable order-of-magnitude estimates, and we are concerned here with the evolution of the shape of the ejecta distribution, not the absolute value of the dust optical depth. The relative production rates of dust of different sizes depend on the mass distribution of the ejecta for a single impact. For this we use

$$n(m)dm = C_m m^{-q_m} dm \quad m_{min} \le m \le m_{max}, \quad (3)$$

where $n(m)dm$ is the number of particles in the mass range m to $m + dm$ and C_m is a normalization constant. Changes in the choice of m_{min} and m_{max} affect only the total amount of dust, not the slope of the distributions. We use $q_m = 1.83$, taken from the experimental results of Asada (1985). The value $q_m = 1.83$ corresponds to a cumulative size index of $b_r = 2.5$, where

$$N(> r) = C_r r^{-b_r} \quad (4)$$

is the cumulative number of dust particles of radius larger than r.

II.2. Evolution of Ejecta Orbits

For an uncharged dust particle in an equatorial orbit about a zero obliquity planet with $e \ll 1$, the combination of radiation pressure and planetary oblateness causes perturbations to the orbit averaged orbital elements (Burns *et al.* 1979, Chamberlain 1979),

$$< \frac{da}{dt} > = 0 \quad (5a)$$

$$< \frac{de}{dt} > = \lambda \sin\tilde{\omega} \quad (5b)$$

$$< \frac{d\tilde{\omega}}{dt} > = \frac{\lambda}{e}\cos\tilde{\omega} + \dot{\tilde{\omega}}_{J_2}, \quad (5c)$$

where $\lambda \equiv \frac{3}{2} hf/\mu$, h is the specific angular momentum, f is the acceleration due to the solar radiation perturbation, $\mu = GM_{plan}$, $\tilde{\omega}$ is the longitude of periapse, and $\dot{\tilde{\omega}}_{J_2}$ is the rate of change of the apse due to the oblateness of the planet. The specific angular momentum is $h = \sqrt{a\mu(1 - e^2)}$, and the precession due to the oblateness of the planet is (Danby 1988)

$$\dot{\tilde{\omega}}_{J_2} = \frac{3}{2}\omega_k J_2 \left(\frac{R_{plan}}{a}\right)^2 \propto a^{-7/2}, \quad (6)$$

where J_2 is the gravitational quadrupole moment of the planet, $\omega_k = \sqrt{\mu/a^3}$ is the Kepler angular velocity, R_{plan} is the radius of the planet, and a is the semimajor axis of the particle's orbit. The acceleration of a particle due to radiation pressure, f, is given by

$$f = \frac{S_o Q_{pr} \pi r^2}{cD^2 m} = \frac{3 S_o Q_{pr}}{4cD^2 \rho r}, \quad (7)$$

where $S_o = 1.36 \times 10^6$ erg sec^{-1} cm^{-2} is the solar radiation energy flux at 1 AU, Q_{pr} is a dimensionless scattering efficiency factor (of order unity for $r \gtrsim 1$ μm), D is the distance from the sun in astronomical units, c is the speed of light, and ρ is the dust particle density.

Horanyi and Burns (1991) solved Eqs. (5) analytically for a dust particle initially on a circular orbit, yielding the following expression for periodic eccentricity evolution:

$$e(t) = \frac{\lambda}{\dot{\tilde{\omega}}_{J_2}} \sqrt{2(1 - \cos\dot{\tilde{\omega}}_{J_2} t)}. \quad (8)$$

For a particle of mass m, the maximum perturbed eccentricity is

$$e_{max} = \frac{2\lambda}{\dot{\tilde{\omega}}_{J_2}}. \quad (9)$$

Radiation pressure and oblateness also cause a change in longitude of periapse. We have assumed a random distribution of apses since we consider continuous production of ejecta as the moon orbits the planet.

II.3. Collision Frequencies

To determine the collision frequencies between orbiting dust particles and the satellite we have used expressions for impact rates of planetesimals onto protoplanets derived by Greenberg *et al.* (1991). These impact rates correspond to three "regimes" which represent differences in collision rates based on a comparison of the random motion of a particle to the gravitational influence of the satellite. In our model, particles are always in either Regime A or Regime B of Greenberg *et al.* (1991).

When random motion is the dominant mechanism for determining approach velocities to the satellite, a two-body approximation may be used to derive an expression for the number of particles impacting the satellite per unit time. This is the defining condition for Regime A, and the corresponding impact rate is (Greenberg *et al.* 1991)

$$I_A \approx R^2\left(1 + \frac{V_e^2}{n^2 a^2((5/8)e^2 + i^2)}\right) \frac{na((5/8)e^2 + i^2)^{1/2}\sigma}{i}, \quad (10)$$

where V_e and n are the escape velocity and mean orbital motion of the satellite, respectively, i is the inclination of the dust particle, and σ is the surface number density of dust. We define the surface number density of dust particles of a given radius to be $\sigma = n(r)/(2\pi a^2 e_{max})$, where e_{max} is given by Eq. (9). The Regime A collision frequency is simply a particle-in-a-box collision frequency, enhanced by two-body gravitational focusing. The quantity $na\sqrt{5/8e^2 + i^2}$ is the random velocity of a particle in the frame of the satellite. Thus, Eq. (10) can be reduced to, approximately, $I_A = V_{ran}R^2 n(r)/V$, where V is the volume of the particle swarm.

For low random velocities the particle-in-a-box relation breaks down. If the particles' eccentricities are small, impacts with the satellite occur mainly due to gravitational perturbations by the satellite. The relative velocity of such impacts is controlled by the differential Keplerian velocities of the particles and the satellite, rather than by initial random motion. In this case, the rate of collisions of ejecta with the satellite is

$$I_B \approx R^2\left(1 + \frac{0.56V_e^2}{R_H^2 n^2(2\nu^{-1/15} - 1.27)}\right) \frac{3.2nR_H\nu^{-1/15}\sigma}{ai}, \quad (11)$$

where R_H is the satellite's Hill radius, and ν is the ratio of the satellite mass to the planet mass. This is defined as Regime B by Greenberg *et al.* (1991). We use as a criterion for the boundary between Regimes A and B, $ea = 2.3\ R_H$. The coefficient may be as large as 2.5 (Greenberg *et al.* 1991). A larger leading coefficient would make our size distribution steeper at slightly smaller particle sizes than what we find below. It should be noted that the collision frequencies given by Eqs. (10) and (11) are analytic approximations which agree well with numerical Monte Carlo results (e.g., Greenzweig and Lissauer 1990) for $ea \ll 2.3R_H$ and $ea \gg 2.3R_H$ (see Greenberg *et al.* 1991, Fig. 5). The transition between Regime A and B is actually a gradual one which occurs over an order-of-magnitude in eccentricity values (Greenberg *et al.* 1991). By treating this transition as an immediate one which occurs at $ea = 2.3R_H$, we are calculating collision rates which are approximations to the actual rates for an order-of-magnitude in eccentricity surrounding this boundary. However, since the steepening effects we observe extend over two orders-of-magnitude in eccentricity to one side of this boundary, the general character of the steady-state distributions we find in this study would not be significantly changed by a more exact numerical model for collision rates.

For situations where the swarm of particles is flattened compared to the vertical cross section of the satellite, the collision frequency would be given by the Greenberg *et al.* (1991) Regime C expression. We allow for Regime C collision frequencies, but for the results presented here no particles are ever in that regime. This is expected given the small physical cross section of the moons considered here and the relatively large vertical extent of planetary dust rings.

As an alternative to the Greenberg *et al.* (1991) collision frequencies we also did simulations using an Öpik formula. Specifically, we use (Kessler 1981)

$$I_K = \frac{V_{ran}\pi R^2(1 + (V_e/V_{ran})^2)}{2\pi^3 a_{moon} a \sin i \sqrt{(a_{moon} - q)(q' - a_{moon})}}. \quad (12)$$

This is identical to Öpik's (1951) result for impact rates onto a target in a circular equatorial orbit. The quantities q and q' are the periapse and apoapse distance of the dust particle, respectively. Eq. (12), like Eq. (10), is basically a particle-in-a-box collision frequency. It is only appropriate when the random velocity of the colliding particles is larger than velocity perturbations caused by gravitational encounters with the largest body. Thus, Eq. (12) is not adequate to model all the particles in our simulation. It does provide a check on the specific form adopted for the particle-in-a-box collision frequency of Eq. (10).

II.4. Model Summary

In this simulation, the satellite is on a circular orbit and all dust ejecta produced during an impact are assumed to escape. For the ~10-km-radius moons considered here

this is a reasonable approximation. We assume that ejected dust particles occupy initially circular orbits; this assumption has no effect on the equilibrium size distribution of the ejecta since the perturbations we consider here are periodic. The semimajor axes of the particles are randomly distributed between $a - R$ and $a + R$; similarly, particle inclinations are randomly distributed between 0 and R/a. These conventions are consistent with particles ejected from the surface of the satellite on initially circular orbits. The collision frequencies given in Eqs. (10) and (11) are averages over the satellite's entire accretion "feeding zone," which encompasses a range in semimajor axis of about $a - 3R$ to $a + 3R$ for Adrastea. Trials with dust particles' orbital radii randomly distributed over this broader semimajor axis range produced the same equilibrium dust distributions as those using the narrower range.

The evolution of the size distribution of the ejecta is followed using a logarithmic mass vector, with each mass "bin" of this vector convering a factor of two in mass. A particle in a given mass bin also has a phase in its periodic eccentricity cycle. Each mass bin is therefore subdivided into eccentricity bins which span the range of eccentricities for particles in that mass bin. Newly ejected particles are created at zero phase, i.e. with $e = 0$. At every time step, a new eccentricity for each eccentricity bin in each mass bin is calculated from Eq. (8), particles are added to the system according to Eq. (1), and mass is removed from the system as particles collide with the satellite (Eqs. (10)–(11) or Eq. (12)). We assume that any particles that collide with the satellite are lost from the system. Inclination and semimajor axes are kept constant with time. A constant value for i is a good approximation for the zero-obliquity case, in which radiation pressure does not affect orbital inclination. Particle inclinations will be modified by collisions between dust particles; this is unimportant for this work as characteristic times for interparticle collisions in low optical depth dust rings are much greater than the time scales considered here.

III. RESULTS

We calculate steady-state size distributions for Adrastea, a small satellite located within Jupiter's main ring at $1.8R_J$. Figure 1 shows the ejecta size distributions at approximately 6-month intervals, as well as the ejecta source size distributions for comparison, using the Greenberg *et al.* collision frequencies. Steady-state was reached in approximately 12 years. Figure 1 also indicates the logarithmic slopes of three regions of the equilibrium size distribution. The logarithmic slopes derived from our results yield *incremental* power-law indicies, since our simulations record the evolution of an incremental size distribution in terms of discrete, logarithmically spaced bins. Our bin spacing is wide enough so that an incremental size index that is obtained from our results is equivalent to a *cumulative* size index, b_r, as defined in Eq. (4) (Colwell 1993). The slopes indicated in Fig. 1 can therefore be interpreted as cumulative slopes.

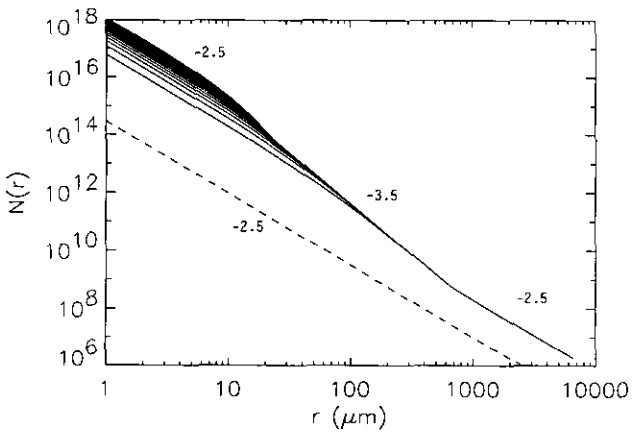

FIG. 1. Dust ejecta size distributions in orbit near Adrastea ($a = 1.29 \times 10^5$ km $= 1.8R_J$, $R = 10$ km). Size distributions are shown at 6-month intervals (solid lines); the earliest interval is the lowest in magnitude and the time for steady-state to be reached is 12 years. The dashed line represents the source distribution added at each time step. The slopes of the distributions are indicated. Particles whose radii are less than approximately 11 μm are in collisional Regime A (Eq. (10)), while larger particles are in collisional Regime B (Eq. (11)).

If orbital modifications due to radiation pressure and planetary oblateness were ignored, the slope of the entire steady-state distribution would be identical to that of the source distribution, since the collision frequencies would be independent of ejecta particle size. The source slope is preserved in two regions of the ejecta distribution in this model: (1) small particles whose eccentricities have been pumped high enough so that the low collisional rates are independent of changes in the eccentricity due to the different particle sizes, and (2) large particles whose eccentricities are all too small to affect collision rates. Region 1 particles are all in the particle-in-a-box collision regime. Region 2 particles are all in the Kepler shear regime (Regime B). Thus, the Öpik formula is appropriate for high-eccentricity particles that preserve the source size distribution. In the interim range of particle sizes, the effects of radiation pressure and oblateness result in size-dependent collision rates leading to a change in the slope of the steady-state size distribution by 1, as seen in Fig. 1.

The steep interim region results from the Region 2 particles colliding more frequently with the satellite than the Region 1 particles. Since these larger particles are removed preferentially, the interim size distribution steepens. The specific region of the size distribution affected is governed by the strength of the perturbations, the orbital radius, and the size of the satellite. Our numerical simula-

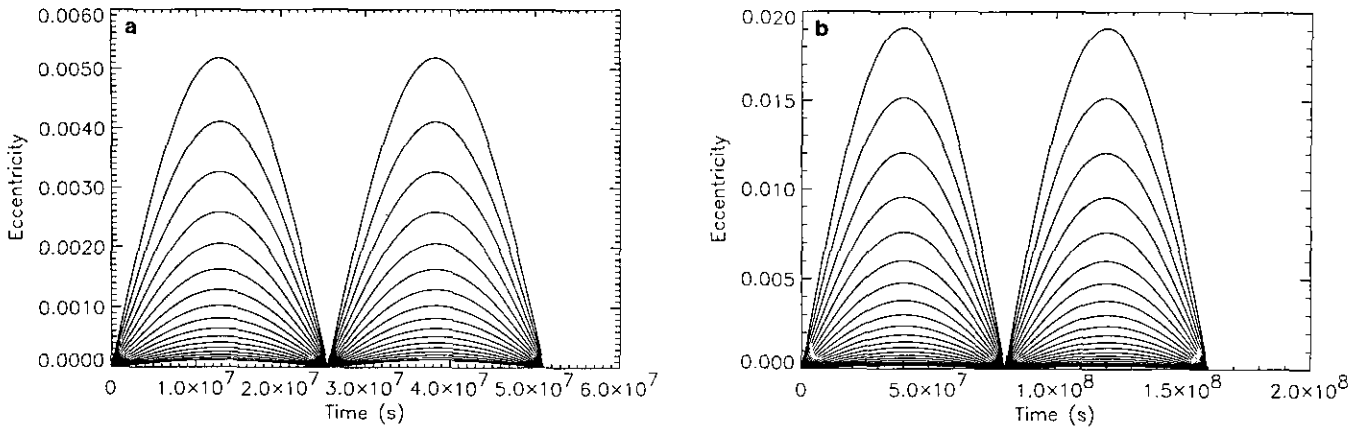

FIG. 2. The eccentricity evolution through two periods at (a) $1.8R_J$ and (b) $2.5R_J$. Each curve represents the eccentricity evolution for a different size bin, the largest amplitude curve for 1-μm particles and the smallest amplitude curve for 1000-μm particles. Equations (9) and (6) can be used to relate the amplitude of (a) and (b).

tions show that the small-size modification to the steady-state distribution begins approximately when $ae_{max} \sim 10R$; similarly the large-end knee in the distribution occurs when $ae_{max} \sim 0.1R$. The modified region is bounded by these limits. Physically, these boundaries reflect the insensitivity of impact rates to particle eccentricity when the epicycle width of a particle's motion, ae_{max}, is either much less than or much greater than the size of the target satellite. If we solve for the particle sizes whose e_{max} values correspond to $10R/a$ and $0.1R/a$ for a given satellite size and location (Eq. (9)), we find that the modified region is located approximately between particles of radius $(1–100)r_{crit}$, where r_{crit} (in cgs units) is

$$r_{crit} \sim \frac{72a^5 Q_{pr}}{RD^2 \rho J_2 R_{plan}^2 M_{plan}}, \tag{13}$$

where R_{plan} is the planet radius and D is in astronomical units. Thus for a satellite in orbit around a given planet, $(1–100)r_{crit}$ is the particle size range where a steepening in the dust ejecta size distribution due to radiation pressure and planetary oblateness would be observed. The small-size "knee" at $r \sim r_{crit}$ is rounded due to the transition between Regime A and Regime B collision rate expressions (Eqs. (10) and (11)), which have different dependences on particle eccentricity. Particles larger than this knee are all in the collisional Regime B.

Figure 2 shows the eccentricity evolution through two periodic cycles for particles ranging in size from 1 to 1000 μm at Adrastea. As seen from Eqs. (6) and (9), Adrastea's relatively short orbital period causes the eccentricity induced by radiation pressure to be small; in contrast, at $2.5R_J$ radiation pressure produces larger amplitude variations, as shown in Fig. 2b.

The effect of radiation pressure and oblateness is to steepen the size power law index of the dust distribution by 1 from that of the source distribution in a limited size regime. Throughout most of the interim region, particle velocities are low enough so that collision rates are determined by Eq. (11). The low-velocity, Regime B impact rate is inversely proportional to the maximum perturbed eccentricity and since $e_{max} \propto 1/r$, the impact rate is proportional to particle radius. Consequently, large dust particles are depleted from the system faster than smaller particles due to their higher collision rates with the satellite. The removal rate of particles of radius r is proportional to (from Eq. (11))

$$\frac{d(n(r))}{dt}_{sink} \propto n(r)r. \tag{14}$$

The supply rate of radius r varies as

$$\frac{d(n(r))}{dt}_{source} \propto r^{-q_r}, \tag{15}$$

where q_r is the differential size power-law index. Equating these two rates yields the steady-state size distribution

$$n(r) \propto r^{-q_r-1}, \tag{16}$$

whose slope is steeper by 1 than the slope of the original source distribution. In Fig. 1, our source size distribution has a cumulative slope of -2.5 and the interim steady-state slope is -3.5. Figure 3 demonstrates the effect of changing the slope of the source distribution on the steady-state distribution.

We have tested our results by using the Öpik collision frequency (Eq. (12)) in place of the Greenberg *et al.* (1991) rates. The steady-state size distribution has a discontinu-

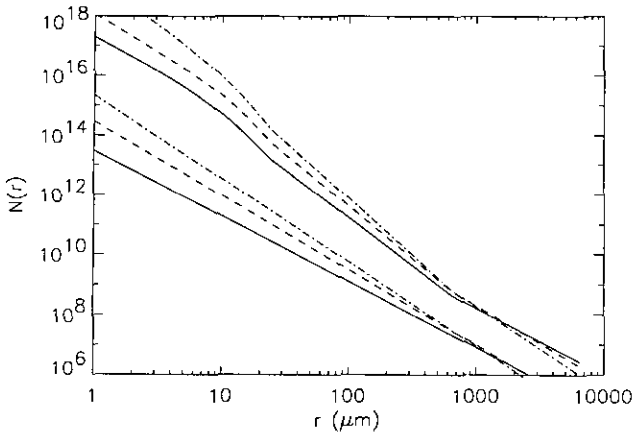

FIG. 3. The steady-state size distribution for Adrastea with three different source size distributions, with cumulative size power-law indices of 2.8 (solid), 2.5 (dashed), and 2.2 (dot–dashed). Particles whose radii are less than approximately 11 μm are in collisional Regime A (Eq. (10)), while larger particles are in collisional Regime B (Eq. (11)).

ity at r_{crit} where the particle-in-a-box approximation breaks down. We have also assigned arbitrary minimum eccentricities to the particle swarm. When the minimum eccentricity is 10^{-3} for Adrastea, the interim region disappears. This is because at that eccentricity all particles are still in Regime A. As the minimum eccentricity is lowered, more particles are allowed to move into the Kepler shear regime and the interim steep size distribution reappears. At a minimum eccentricity of 10^{-4} the interim region extends from r_{crit} to approximately $10r_{crit}$.

DISCUSSION

We have modeled the effect of radiation pressure and planetary oblateness on the orbits of dust particles ejected from small satellites located a few planetary radii from Jupiter. We have examined the steady-state dust distribution resulting from the balance of ejecta production due to micrometeoroid bombardment and dust reimpact with the parent satellite. We find that the orbital perturbations caused by radiation pressure and planetary oblateness cause a characteristic steepening of the steady-state size distribution over that of the source distribution, spanning up to two orders of magnitude in particle radius. The specific size regime affected is a function of the perturbation strength, the orbital radius, the size of the parent satellite, and the minimum eccentricity of the particle swarm. The steady-state size distribution in this regime has a power-law index exactly one steeper than that of the source distribution. We thus propose a possible mechanism for the steepening of a dust size distribution from that of the source ejecta distribution.

The purpose of this work has been to show the effect of two perturbations on the steady-state size distribution of dust ejected from small satellites and ring moons. Other potentially important effects have been neglected by this preliminary work. First, we have neglected all electromagnetic phenomena. The dust particles of greatest interest here are $\gtrsim 10$ μm in radius; the motion of such particles will be gravitationally dominated for reasonable levels of particle charge (Grün *et al.* 1984, Havnes *et al.* 1992). Horanyi and Burns (1991) have recently demonstrated that the orbits of even weakly charged micrometer-sized dust grains can be periodically altered on month time scales due to charge oscillation induced by planetary shadow effects. The inclusion of these effects could potentially alter the results presented here for the smaller dust grains; however, the steady-state size distribution for particles $\gtrsim 10$–100 μm in radius would not be affected.

Our model also does not include the effects of drag processes. Poynting–Robertson and plasma drag cause orbital change on greater time scales than those discussed here. Poynting–Robertson drag time scales for 10-μm particles in orbit around Jupiter are on the order of 4×10^5 years (Burns *et al.* 1984). Plasma drag time scales for 10-μm particles in the main band of the jovian ring (a = 122,800–129,200 km) are on the order of $2 \times 10^{3\pm1}$ years (Burns *et al.* 1984). In certain regions of ring systems, exospheric drag perturbs particle orbits on time scales comparable to the radiation pressure effects discussed here. At the inner edge of the uranian ring system, exospheric drag produces inward radial velocities as great as 10 cm/sec for micrometer-sized particles, corresponding to a crossing time on the order of a few weeks for a 100-km ring (Colwell and Esposito 1990a). Drag processes preferentially remove small particles, resulting in a flattening of the slope of the steady-state size distribution by 1 from that of the initial source distribution. In regions where drag time scales are comparable to that of radiation pressure in the neighborhood of a satellite, the effect of drag processes on the steady-state distribution would thus be exactly offset in the size regime affected by radiation pressure.

Equations (5) assume zero inclination or that the orbital plane of the dust particle is coplanar with the orbital plane of the planet about the Sun. For ring systems found in the equatorial plane of planets with a significant obliquity, the solar radiation pressure will also have a component normal to the ring plane, which will produce periodic changes in inclination as well as eccentricity variations. The effects of inclination will be significant for all ring systems except for that of Jupiter. Recently, Hamilton (1992) has derived radiation pressure perturbation equations valid for all obliquities. A significantly more sophisticated model could include initial distributions of semimajor axis, inclination, and eccentricity for ejected particles.

For low-eccentricity orbits, gravitational perturbations

by the satellite result in either impact with the satellite or scattering. Here we have assumed that such perturbations always result in impact with the satellite, and thus do not affect the eccentricity distribution of the dust ejecta swarm. In reality, some percentage of the particles in the modified regime of the size distribution will have their eccentricities excited during a "near miss" with the satellite. The magnitude of this perturbed eccentricity is independent of dust particle mass. Particles which are scattered onto more eccentric orbits due to the satellite's perturbation will cause a flattening of the steady-state slope in the modified region. However, because the ratio of the Hill radius to the physical radius of a satellite near a ring system is typically small (~1.3 for Adrastea), physical collisions are more likely than scatterings during close encounters. If minimum eccentricities are as high as 10^{-3} for Adrastea, the steepening effect disappears. The magnitude of the minimum eccentricity is controlled, at least in part, by the strength of the gravitational perturbations on the dust by the parent object(s). For Saturn's G ring, where a moonlet belt of sub-kilometer-sized objects has been hypothesized as the source of the dust there (Showalter and Cuzzi 1993), this effect could be important. The small moonlets would excite small minimum eccentricities, and the dust particles would be in a collisional balance between micrometeoroid production and sweep up by the moonlets and on low-eccentricity orbits. This moonlet belt model is the currently favored explanation for the continued existence of dust rings at each of the giant planets. The mechanism described here for steepening dust size distributions may operate at different degrees of efficiency at each dust ring, with obliquity, proximity to the Sun, and size distribution of the moonlets all playing roles. More detailed simulations of the collisional balance of dust within a moonlet belt and in the vicinity of small satellites are necessary to determine the importance of this effect on the size distributions of dust in planetary dust rings.

ACKNOWLEDGMENTS

This research was supported in part by the Neptune Data Analysis Program, NAGW-2404, and the Patricia Roberts Harris Fellowship program. We thank Larry Esposito and Glen Stewart for helpful comments and suggestions. We also thank Dave Kary and Doug Hamilton, whose speedy and helpful reviews were much appreciated.

REFERENCES

ASADA, N. 1985. Fine fragments in high-velocity impact experiments. *J. Geophys. Res.* **90,** 12445–12453.

BANASZKIEWICZ, M., AND W. H. IP 1991. A statistical study of impact ejecta distribution around Phobos and Deimos. *Icarus* **90,** 237–253.

BURNS, J. A., P. L. LAMY, AND S. SOTER 1979. Radiation forces on small particles in the Solar System. *Icarus* **40,** 1–48.

BURNS, J. A., M. R. SHOWALTER, J. N. CUZZI, AND J. B. POLLACK 1980. Physical processes in Jupiter's ring: Clues to its origin by Jove! *Icarus* **44,** 339–360.

BURNS, J. A., M. R. SHOWALTER, AND G. E. MORFILL 1984. Ethereal rings. In *Planetary Rings* (R. Greenberg and A. Brahic, Eds.), pp. 200–272. Univ. of Arizona Press, Tucson.

CHAMBERLAIN, J. W. 1979. Depletion of satellite atoms in a collisionless exosphere by radiation pressure. *Icarus* **39,** 286–294.

COLWELL, J. E., AND L. W. ESPOSITO 1990a. A numerical model of the uranian dust rings. *Icarus* **86,** 530–560.

COLWELL, J. E., AND L. W. ESPOSITO 1990b. A model of dust production in the Neptune ring system. *Geophys. Rev. Lett.* **17,** 1741–1744.

COLWELL, J. E. 1993. Power-law confusion: You say incremental, I say differential. Submitted for publication.

CUZZI, J. N., AND R. H. DURISEN 1990. Bombardment of planetary rings by meteoroids: General formulation and effects of Oort cloud projectiles. *Icarus* **84,** 467–501.

DANBY, J. M. A. 1988. *Celestial Mechanics,* 2nd. ed. Willmann–Bell, Richmond, VA.

GREENBERG, R., W. F. BOTTKE, A. CARUSI, AND G. B. VALSECCHI 1991. Planetary accretion rates: Analytical derivation. *Icarus* **94,** 98–111.

GREENZWEIG, Y., AND J. J. LISSAUER 1990. Accretion rates of protoplanets. *Icarus* **87,** 40–77.

GRÜN, E., G. E. MORFILL, AND D. A. MENDIS 1984. Dust–magnetosphere interactions. In *Planetary Rings* (R. Greenberg and A. Brahic, Eds.), pp. 275–332. Univ. of Arizona Press, Tucson.

HAMILTON, D. P. 1992. Motion of dust in a planetary magnetosphere: Orbit-averaged equations for oblateness, electromagnetic, and radiation forces with application to Saturn's E ring. *Icarus* **101,** 244–264.

HAVNES, O., G. E. MORFILL, AND F. MELANDSO 1992. Effects of electromagnetic and plasma drag forces on the orbit evolution of dust in planetary magnetospheres. *Icarus* **98,** 141–150.

HORANYI, M., AND J. A. BURNS 1991. Charged dust dynamics: Orbital resonance due to planetary shadows. *J. Geophys. Res.* **96,** 19,283–19,289.

JUHÁSZ, A., M. TÁTRALLYAY, G. GÉVAI, AND M. HORÁNYI 1993. On the density of the dust halo around Mars. *J. Geophys. Res.* **98,** 1205–1211.

KESSLER, D. J. 1981. Derivation of the collision probability between orbiting objects: The lifetimes of Jupiter's outer moons. *Icarus* **48,** 39–48.

MORFILL, G. E., E. GRÜN, AND T. V. JOHNSON 1983. Saturn's E, G, and F Rings: Modulated by the Plasma Sheet. *J. Geophys. Rev.* **88,** 5573–5579.

ÖPIK, E. J. 1951. Collision probabilities with the planets and the distribution of interplanetary matter. *Proc. R. Irish Acad.* **54,** 165–199.

SOTER, S. 1971. The dust belts of Mars. *Cornell Center Radiophys. Space Phys. Rept.* 472.

SHOWALTER, M. R., AND J. N. CUZZI 1993. Seeing ghosts: Photometry of Saturn's G ring. *Icarus* **103,** 124–143.